An Expanded Palette of Fluorescent COS/H_2S-Releasing Donors for H_2S Delivery, Detection, and In Vivo Application

Kaylin G. Fosnacht, Jonathan Dorogin, Payton M. Jefferis, Marian H. Hettiaratchi, and Michael D. Pluth*

[a] K. G. Fosnacht, J. Dorogin, P. M. Jefferis, Dr. M. H. Hettiaratchi, Dr. M. D. Pluth
Department of Chemistry and Biochemistry, Materials Science Institute, Knight Campus for Accelerating Scientific Impact, Institute of Molecular Biology, University of Oregon, Eugene, OR, 97403 United States. Email: pluth@uoregon.edu

Abstract: Hydrogen sulfide is an important reactive sulfur species that is involved in many biological functions, and H_2S imbalances have been indicated as a potential biomarker for various diseases. Different H_2S donors have been developed to deliver H_2S directly to biological systems, but few reports include donors with optical responses that allow for tracking of H_2S release. Moreover, donor systems that use the same chemistry to deliver H_2S across a palette of fluorescent responses remain lacking. Here we report five thiol-activated fluorescence turn-on COS/H_2S donors that utilize blue, yellow, orange, red, and near infrared-emitting dyes functionalized with an H_2S-releasing sulfenyl thiocarbonate scaffold. Upon treatment with thiols, each donor provides a fluorescence turn-on response (3–310-fold) and high H_2S release efficiencies (>60%). Using combined electrode and fluorescence experiments, we directly correlate the measured H_2S release with the fluorescence response. All donors are biocompatible and release H_2S in live cell environments. In addition, we demonstrate that the NIR donor allows for H_2S release tracking after subcutaneous injection in live rats, which to the best of our knowledge is the first *in vivo* tracking of fluorogenic H_2S release in non-transparent organisms.

Introduction

Reactive sulfur species (RSS), such as thiols, polysulfides, hydrogen sulfide (H_2S), and persulfides are important small molecules relevant to human health. H_2S is a known gasotransmitter, generally defined as an endogenously produced and membrane permeable gaseous molecule that is highly involved in biological pathways, cellular signaling, and cell function.[1-2] More recently, H_2S has been shown to be intertwined with various processes including cell apoptosis, cellular metabolism, endoplasmic reticulum stress, vasorelaxation, and oxidative stress.[3-8] For example, the observed vasorelaxation from H_2S stems from the reaction of H_2S with oxidized cysteine (Cys) residues of ATP-sensitive potassium channels to produce persulfides, which opens these channels and results in downstream effects of decreasing blood pressure.[9-11] As the fundamental understanding of H_2S and other RSS in biology continues to expand, tools are needed to monitor and perturb RSS in living systems to advance investigations into the biological functions of RSS.

Inspired by the beneficial biological effects associated with H_2S, a variety of compounds that release H_2S when activated by specific stimuli, such as light, enzymes, or nucleophiles, have been developed.[12-14] The direct addition of H_2S gas or sulfide salts to biological media results in an immediate bolus of H_2S delivery, which typically lacks physiological relevance.[15] In contrast, donor compounds that release H_2S in response to specific stimuli or at consistent, low levels over time mimic endogenous H_2S production. H_2S donors can be used to release H_2S in cellular environments, but there are few non-destructive methods to monitor H_2S release from such compounds, and it remains impractical to use fluorescent H_2S probes in these contexts because the probes consume the H_2S released by the donor.[16-18] Analyte replacement H_2S probes that release H_2S upon probe activation may offer one approach to overcome these challenges, but such systems do not result in full H_2S replacement and are useful as H_2S detection rather than delivery systems.[19-21] To more directly remedy this problem, small molecule H_2S donors that release both H_2S and a fluorescent marker provide an important tool to track temporal H_2S release in real time.

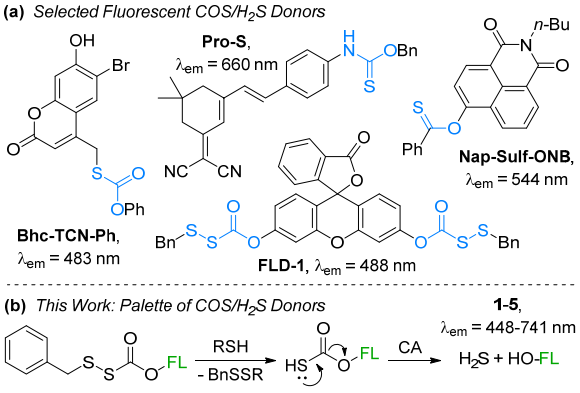

Figure 1. (a) Selected small molecule fluorogenic COS/H_2S donors that incorporate different fluorophores and H_2S-releasing scaffolds. (b) Activation mechanism for COS/H_2S and fluorophore (FL) release from donors **1**–**5**.

Fluorogenic H_2S donors with direct H_2S-releasing scaffolds, such as trisulfides and activated thioethers, or indirect COS/H_2S-releasing scaffolds, such as thioesters, thiocarbamates, thiocarbonates, and sulfenyl thiocarbonates, have been reported previously (Figure 1a).[19, 22-37] Indirect COS/H_2S donors function by the intermediate release of COS, which is rapidly converted to H_2S in cellular environments by the enzyme carbonic anhydrase (CA). These COS/H_2S donor scaffolds enable easy modification via addition of an alcohol or amine-modified fluorescent dye. From the available approaches for H_2S delivery coupled with a fluorescence response, there are a number of limitations. First, fluorogenic donors that utilize the same H_2S release chemistry across the palette of fluorophores have not been reported, which

makes it difficult to compare the outcomes of different platforms across a series of samples. In addition, no near infrared (NIR) donors with emissions above 700 nm have been developed, which further limits applications to *in vivo* use and imaging. Furthermore, fluorogenic donors have not yet been demonstrated in subcutaneous imaging in non-transparent organisms, which is a key step in advancing the biocompatibility of this important class of compounds. These as well as other factors are major limitations for translating this chemistry into more complex *in vivo* environments. Herein, we expand the palette to include fluorescent H_2S donors spanning the emission spectrum to include blue, yellow, orange, red, and NIR (>700 nm) donors, and demonstrate their use both in cell culture and subcutaneous *in vivo* animal work to advance this important class of compounds for studying H_2S in biology (Figure 1b).

Results and Discussion

H_2S donors based on the perthiocarbonate scaffold, also referred to as a sulfenyl thiocarbonate, were previously utilized by our group to develop a fluorescein-based H_2S donor.[38] This study showed that the perthiocarbonate scaffold can be activated by thiols to result in COS/H_2S release and concurrent fluorescent turn-on response. Functionally, these donors undergo general activation by thiols rather than a one specific activating analyte, which is beneficial to the donor design since no single species will be depleted, and the overall RSS redox state in complex biological systems is not significantly perturbed. Previous work provided a proof-of-concept for fluorogenic H_2S delivery and fluorescence responses, but neither chromophore diversification nor translation to *in vivo* applications were reported. To bridge this gap, we prepared different fluorogenic H_2S donors using fluorophores that spanned different emissive regions of the visible and NIR spectrum. Using these commercially or synthetically available fluorophores, we treated each precursor with readily prepared ((benzyl)dithio)carbonyl chloride in the presence of DIPEA to afford the corresponding donors **1**–**5** in moderate to high yields (34–98%, Figure 2).[38-42] All compounds were characterized by ^{1}H and ^{13}C(^{1}H) NMR spectroscopy and mass spectrometry.

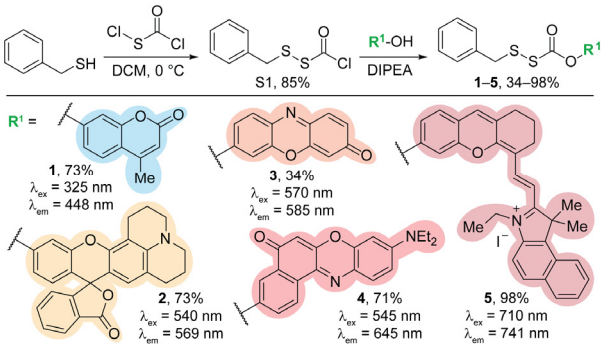

Figure 2. Synthetic pathway of fluorogenic COS/H_2S donors **1**–**5.**

Following the synthesis of donors **1**–**5**, we next investigated the spectroscopic properties of each system in phosphate buffered saline (PBS) buffer (10 mM, pH 7.4). For donors **1**–**5**, alkylation of the alcohol significantly quenches the fluorescence and shifts the absorption from the original fluorophore (Table 1, Figures S5–S9). For donors **1**–**3** that contain smaller conjugated systems, this alkylation completely abolishes the fluorescence, whereas for larger, more conjugated donors **4** and **5**, this alkylation shifts the absorbance and results in residual minor fluorescence at a shifted wavelength. Based on the documented low solubility and fluorescence of Nile Red, we used cetyltrimethylammonium bromide (CTAB, 1.0 mM) to increase solubility and fluorescent response of **4** and **5** for *in situ* measurements.[40, 43-44] Overall, all synthesized donors displayed significantly decreased fluorescence when compared to the parent fluorophore, which matched our design principle in designing fluorogenic COS/H_2S releasing motifs.

After evaluating the photophysical properties of **1**–**5**, we next investigated the fluorescence turn-on and H_2S release from each donor. To carry out these experiments, we used 10 μM of each donor in the presence of CA (25 μg mL^{-1}) and 10 equiv. of Cys (100 μM) and monitored the fluorescence response and H_2S release over a 120-minute period (Figure 3, S17–S21, and S23–27). We chose to use an H_2S responsive electrode for these measurements to have better time resolution than other H_2S measurement techniques. Importantly, this approach also allowed for the direct comparison of H_2S release and fluorescence response with high temporal resolution, which to the best of our knowledge has not been investigated previously.

Table 1. Spectroscopic properties of donors **1**–**5** and the corresponding fluorophores.[39, 45-46]

Compound	Parent Fluorophore				COS/H_2S Donor			
	λ_{max} (nm)	λ_{em} (nm)	ε (M^{-1} cm^{-1})	Φ[a]	λ_{max} (nm)	λ_{em} (nm)	ε (M^{-1} cm^{-1})	Φ[a]
1	325	448	14,900	0.36	–	–	–	–
2	540	569	29,300	0.46	–	–	–	–
3	570	585	56,000	0.74	–	–	–	–
4[b]	545	645	5,100 55,000[c]	0.08 0.67[c]	500	640	4,800	0.02
5[b]	710	744	54,000	0.12	610	737	27,000	0.06

[a] The Φ of **4** and **5** is referenced to rhodamine 101 and 1,1′,3,3,3′,3′-hexamethylindotricarbocyanine iodide, respectively. [b] In 1.0 mM CTAB in 10 mM PBS buffer (pH 7.4). [c] Measured in EtOH.

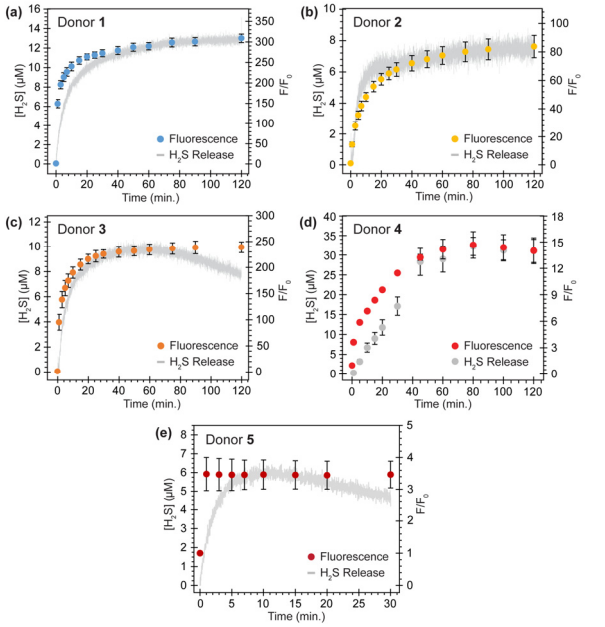

Figure 3. Fluorescence response and H_2S release from COS/H_2S donors (a) **1**, (b) **2**, (c) **3**, (d) **4**, and (e) **5**. General conditions: **1**–**3**, **5** (10 μM) with Cys (100 μM) and CA (25 μg mL^{-1}) in PBS buffer (10 mM, pH 7.4) at 25 °C. Donor **4**: (50 μM) with Cys (500 μM) and CA (50 μg mL^{-1}) in PBS buffer (10 mM, pH 7.4) at 25 °C. The experiments were performed in triplicate and results are expressed as mean ± SD (n = 3).

For donor **1**, we observed a 310-fold fluorescence turn-on and quantitative H_2S release. For donors **2** and **3** we observed an 84-fold fluorescence turn-on and 7.1 μM (71%) H_2S release, and 240-fold fluorescent turn-on and 9.7 μM (97%) H_2S release, respectively. We found that that donor **4** was incompatible with the H_2S-selective electrode due to unanticipated interactions between the Nile Red derivative and the semi-permeable electrode membrane, so H_2S release was measured using the methylene blue H_2S assay. Based on the lower sensitivity of the methylene blue method than the electrode-based experiments, we chose to use higher donor concentrations to ensure accurate H_2S measurement at early reaction time points (50 μM donor, 0.5 μM Cys, and 50 μg mL^{-1} CA), which also required 20% MeCN co-solvent to ensure full solubility of the released fluorophore. Under these conditions, donor **4** resulted in a 15-fold fluorescence turn-on and 32.3 μM H_2S (65%) released over 120 minutes. For NIR donor **5**, we observed H_2S release of 6.0 μM (60%) over 30 minutes whereas the fluorescence instantaneously increased 4-fold after Cys addition. At sub-stoichiometric amounts of cysteine, an increase in the fluorescent response of donor **5** with addition of cysteine was observed, confirming that fluorescence of this donor is dependent on thiol concentration (Figure S22). Overall, donors **1**–**3** released H_2S at a similar rate with maximum H_2S release observed after 40 minutes, whereas the more red-shifted donors **4** and **5** released H_2S on very different timescales with maximum H_2S release being observed after 80 and 10 minutes, respectively.

As shown in Figure 3, the fluorescent donors efficiently release H_2S with a concomitant fluorescence response, which is consistent with the donor design. When comparing the electrode versus fluorimeter responses in **1**–**3**, as well as the fluorescence versus methylene blue response for **4**, we noticed slight differences in rates for these two processes. For donors **1** and **3**–**4**, the fluorescence turn-on increases at a faster rate than H_2S production at early timepoints, whereas the opposite is observed for donor **2**.

For donors **1**, **3**, and **4**, we attribute this trend to a longer lifetime of the thiocarbonate intermediate generated upon initial disulfide cleavage. Notably, each of these three donors has a fully conjugated π-system that could stabilize the thiocarbonate intermediate and potentially provide a fluorescent intermediate, which would account for the observed small lag time in COS/H_2S release upon disulfide cleavage. In contrast, the lactone form of **2** reduces the overall conjugation of the system in the non-fluorescent state, which may lead to a shorter thiocarbonate intermediate lifetime prior to COS/H_2S release. Attempts to observe these transient thiocarbonate intermediates directly have proven unsuccessful, but we do note that Chakrapani and co-workers did observe a presumed arylthiocarbonate intermediate by HPLC from an esterase-activated *S*-alkyl thiocarbonate previously, which would be consistent with the above hypothesis.[47]

Donor **5** releases H_2S the fastest of the presented donors, with full H_2S release being observed after only about 10 minutes. Consistent with the observed instantaneous fluorescence turn-on, this fast H_2S release rate could be due to either the donor releasing COS rapidly, which exceeds the rate of CA conversion of COS to H_2S, or the donor being activated to form a fluorescent intermediate. With the exception of donor **5** that releases H_2S very quickly, donors **1**–**4** release H_2S over a longer time period with full fluorescence turn-on and H_2S release observed after 40–80 minutes (Figure 3). Additionally, donors **1**–**3** result in large fluorescence turn-on responses (84–310-fold turn-on), and the more red-shifted donors **4** and **5** result in lower fluorescence turn-on responses (4–15-fold turn-on). This lower fluorescence response is likely due to the donor compounds themselves having minimal but observable latent fluorescence, as discussed previously. Overall, donors **1**–**5** resulted in concomitant fluorescence turn-on response and H_2S release with high COS/H_2S release efficiencies (>60%) observed.

After establishing the correlation of H_2S release and fluorescence response from these donors, we next investigated the activation of these donors by other biologically relevant sulfur, nitrogen, and oxygen species (Figure 4 and S28). For these selectivity experiments, we used donor **1** due to the high H_2S release efficiency, sizeable fluorescence response, and temporal correlation between fluorescence response and H_2S release. We first treated **1** (10 μM) with biologically relevant thiols (100 μM) including Cys, homocysteine (Hcy), *N*-acetyl cysteine (NAC), glutathione (GSH), and penicillamine (Pen). After 120 minutes, all thiols generated a fluorescence response from **1**. This activation of the donor by various biological thiols highlights that application of these donors to biological systems will not deplete one specific species and not greatly affect RSS. We also found that sulfite (SO_3^{2-}) generated a fluorescence turn-on, which is consistent with the ability of SO_3^{2-} to reduce disulfides.[48] Incubation of **1** with serine (Ser), lysine (Lys), glycine (Gly), oxidized glutathione (GSSG), superoxide (O_2^-), hydrogen peroxide (H_2O_2), or sulfate (SO_4^{2-}) failed to produce a significant fluorescent response.

Donor **1** was also activated by both porcine liver esterase (PLE, 1.0 U mL^{-1}) and CA (25 μg mL^{-1}), which was previously observed with other sulfenyl thiocarbonates and further supports the general activation of this delivery platform.[49] Although donor **1** is less stable in the presence of esterases, the rate of hydrolysis by CA is slower than the reactivity of Cys, with the analytes taking 120 minutes and 30 minutes to fully activate **1**, respectively (Figure S29). Additionally, the degradation of **1** by CA is likely significantly amplified by ester hydrolysis of the donor releasing a thiol byproduct, which increases the rate of donor activation and is magnified in the closed system of the cuvette. In addition to biological species, these donors were confirmed to be photostable, with minimal fluorescence turn-on being observed over 30 minutes of excitation (Figure S30 and S31).

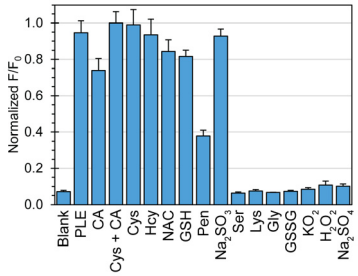

Figure 4. Fluorescence turn-on of donor **3** (10 μM) upon incubated with analytes (100 μM) for 120 minutes in PBS buffer (10 mM, pH 7.4). Conditions from left to right: blank, PLE, CA, Cys + CA, Cys, Hcy, NAC, GSH, Pen, SO_3^{2-}, Ser, Lys, Gly, GSSG, O_2^-, H_2O_2, and SO_4^{2-}. λ_{ex} = 350 nm, λ_{em} = 370–600 nm, T = 25 °C, slit width = 2 nm. The experiments were performed in triplicate and results are expressed as mean ± SD (*n* = 3).

We next investigated whether donors **1**–**5** were compatible with live cell imaging using HeLa cells and co-incubation with the H_2S responsive and cell-trappable probe CT-MeRhoAz to detect H_2S in a cellular environment. We chose to use CT-MeRhoAz because its spectral window does not overlap with donors **1**–**5** and the cell trappability increases signal retention.[50] HeLa cells were incubated with either the vehicle, H_2S probe, H_2S donor, or both the H_2S probe and H_2S donor for 20 minutes and then imaged by fluorescence microscopy (Figure S32–S36). Cells were also co-incubated with the nuclear dye NucRed (for **1**) or Hoechst 33342 (for **2**–**5**). For each of the donors investigated, we observed a fluorescence response from the donor that correlated to the released fluorophore both in the presence and absence of CT-MeRhoAz. These results demonstrated that these donors function in live cell environments and also confirmed that the probe was not producing a false fluorescent response of the donors due to channel bleed through. When the experiments were repeated in the presence of CT-MeRhoAz, we also observed a significant fluorescent response of the H_2S probe that was only observed in the presence of the COS/H_2S (Figure 5). Taken together, these results confirm that donors **1**–**5** release H_2S in a cellular environment, and that the H_2S release can be tracked by fluorescence microscopy.

Based on the efficacy of these donors in live cell environments, we next wanted to translate this donor approach to live animal investigations. We chose to focus on NIR donor **5**, which should have significantly better tissue penetration than donors **1**–**4**. For live animal experiments, donor **5** was loaded into a 2% (w/v) alginate hydrogel before administration into rats. As a proof-of-concept experiment to verify the stability of sulfenyl thiocarbamates in alginate gels we loaded donors **1** and **5** into a 2% alginate hydrogel and monitored the fluorescence over time (Figure S37 and S38). After loading **1** or **5** (10 μM) into the hydrogel and then soaking in PBS buffer (10 mM, pH 7.4) for 20 minutes, minimal fluorescence of the buffer was observed. Addition of buffer containing Cys (100 mM) followed by buffer replacement with agitation both led to an increase in fluorescence response, meaning that the donors are stable in the hydrogel until the addition of Cys activates the donor. To confirm that these donors are still releasing H_2S when loaded into an alginate hydrogel, we directly measured H_2S release from donors **1** and **5** loaded into 2% (w/v) alginate hydrogels using an H_2S selective electrode (Figure S39 and S40). When loaded into the alginate hydrogel, donors **1** and **5** showed slower rates of H_2S release, which is consistent with the expected reduced rate of Cys penetration into the hydrogel to activate the donors. Taken together, these studies show that the donors still respond to thiols with H_2S release and a fluorescent response when loaded into an alginate hydrogel.

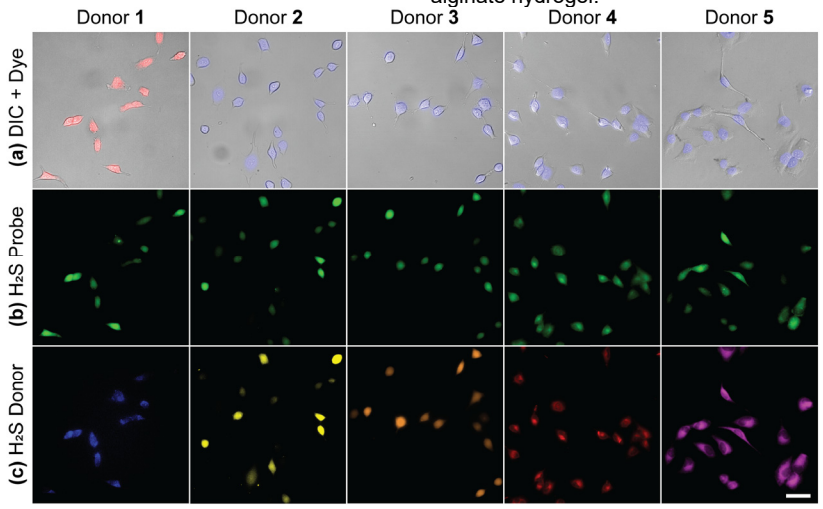

Figure 5. Live-cell imaging of fluorescence turn-on COS/H_2S donors **1**–**5** showing concurrent H_2S release and fluorescence turn-on. (a) Hoechst 33342 (5 μM) or NucRed (2 μM). (b) H_2S probe CT-MeRhoAz (2.5 μM) confirming cellular H_2S release. (c) COS/H_2S donor **1** (50 μM) and **2**–**5** (20 μM). Bar scale: 50 μm.

Having confirmed the stability of the donors in hydrogels, we used donor **5** to investigate whether thiol-mediated donor activation could be observed *in vivo*. Alginate hydrogels were prepared containing either the vehicle (DMSO) or **5** and then injected into the subcutaneous shoulder or hip space of 5–6-week-old male Sprague Dawley rats. After initial imaging using a Perkin Elmer Spectrum In Vivo Imaging System (IVIS), rats were administered sterile GSH via tail vein injection and imaged over 3 hours. As expected, no observable fluorescent signal was observed for either of the alginate gels containing the vehicle with and without GSH administration (Figure S41 and S42). By contrast, inclusion of donor **5** in the alginate hydrogels resulted in a significant fluorescence response (Figure 6, S43, and S44). The fluorescence response is observed both in the absence and presence of exogenous GSH, which we attribute to local activation of the donor by endogenous thiols and esterase/CA enzymes, as was observed in *in vitro* selectivity studies. This fluorescent signal increases appreciably over the first hour, followed by a plateau over the next 2 hours, which is likely due to donor activation followed by diffusion of the fluorophore. These results are highlighted by plotting the average radiant efficiency of regions of interest for all alginate gels (Figure 6b). Overall, these studies confirmed that these donors are compatible with studies in live animals and the fluorescent response can be observed within tissues.

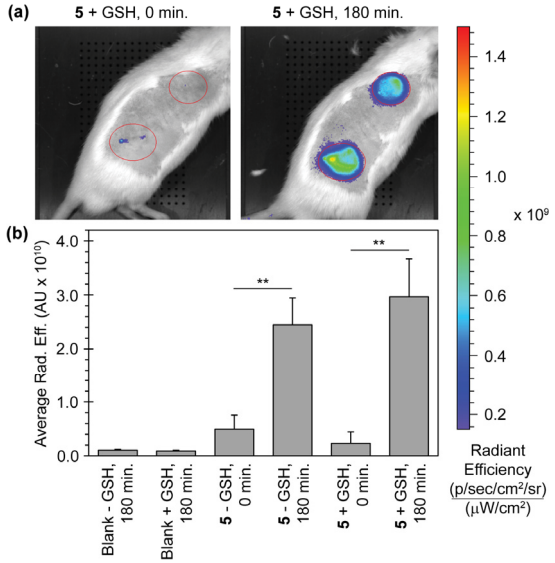

Figure 6. Live rat imaging of fluorescence turn-on COS/H_2S donor **5** loaded into alginate gels. (a) Alginate gels containing **5** (250 μM) before GSH tail vein injection and 180 minutes after GSH injection. Regions of interest are labeled with red circles. (b) Average radiant efficiency of alginate gels loaded with DMSO, DMSO with GSH, donor **5**, and donor **5** with GSH at 0 or 180 minutes. The experiments were performed in quadruplicate and results are expressed as mean ± SD (n = 4). **p < 0.001.

Conclusion

We developed a suite of fluorescent turn-on COS/H_2S donors **1**–**5** that provide fluorescent responses upon release of H_2S across a broad palette of the fluorescence spectrum. Incubation of the donor scaffold with biologically relevant sulfur, nitrogen, and oxygen species confirmed the activation of the donors by a variety of thiol species in addition to sulfite and esterases. This activation profile matches the goal of these donors functioning as slow-releasing COS/H_2S motifs that can be activated by ubiquitous cellular components. By using combined fluorescence and H_2S-responsive electrode experiments, we directly correlated the temporal H_2S release and fluorescence output from each donor. Cell imaging experiments demonstrated that a fluorescence turn-on and H_2S release is observed in a cellular environment for all donors. Additionally, we demonstrated *in vivo* donor activation in live rats using subcutaneous injections of alginate hydrogel containing the NIR donor **5**. Further, this study exemplified that the perthiocarbonate scaffold can be applied to a wide variety of fluorophores with hydroxyl substitutions beyond the specific dyes utilized in this paper. In conclusion, COS/H_2S donors **1**–**5** exemplify the wide application and compatibility of the sulfenyl thiocarbonate scaffold for the development of H_2S donors with various fluorogenic responses and demonstrates the viability of using such donor constructs in both cellular and *in vivo* environments.

Supporting Information

Experimental details, UV-vis, and fluorescence spectra, H_2S release data, cell and animal experiments. The authors have cited additional references within the Supporting Information.

Acknowledgements

Financial support was provided by the NIH (R01GM113030 to MDP). Instrumentation for fluorescence microscopy is supported by the NSF (CHE-1531189)

Keywords: hydrogen sulfide • donor • fluorescent response • reactive sulfur species • rat imaging

[1] R. Wang, *Antioxid. Redox Signal.* **2003**, *5*, 493-501.
[2] K. R. Olson, K. D. Straub, *Physiology* **2016**, *31*, 60-72.
[3] D. Mancardi, C. Penna, A. Merlino, P. Del Soldato, D. A. Wink, P. Pagliaro, *Biochim. Biophys. Acta - Bioenerg* **2009**, *1787*, 864-872.
[4] S. Jha, J. W. Calvert, M. R. Duranski, A. Ramachandran, D. J. Lefer, *Am. J. Physiol. Heart Circ. Physiol.* **2008**, *295*, H801-H806.
[5] X. Cao, L. Ding, Z.-z. Xie, Y. Yang, M. Whiteman, P. K. Moore, J.-S. Bian, *Antioxid. Redox Signal.* **2019**, *31*, 1-38.
[6] M. Fu, W. Zhang, L. Wu, G. Yang, H. Li, R. Wang, *Proc. Natl. Acad. Sci.* **2012**, *109*, 2943-2948.
[7] H. Wei, R. Zhang, H. Jin, D. Liu, X. Tang, C. Tang, J. Du, *Antioxid. Redox Signal.* **2010**, *12*, 1079-1091.
[8] S. Taniguchi, L. Kang, T. Kimura, I. Niki, *Br. J. Pharmacol.* **2011**, *162*, 1171-1178.
[9] W. Zhao, J. Zhang, Y. Lu, R. Wang, *EMBO J.* **2001**, *20*, 6008-6016.
[10] B. Jiang, G. Tang, K. Cao, L. Wu, R. Wang, *Antioxid. Redox Signal.* **2010**, *12*, 1167-1178.
[11] E. Dongó, G. Beliczai-Marosi, A. S. Dybvig, L. Kiss, *Nitric Oxide* **2018**, *81*, 75-87.
[12] Z. J. Song, M. Y. Ng, Z.-W. Lee, W. Dai, T. Hagen, P. K. Moore, D. Huang, L.-W. Deng, C.-H. Tan, *MedChemComm* **2014**, *5*, 557-570.
[13] C. M. Levinn, M. M. Cerda, M. D. Pluth, *Antioxid. Redox Signal.* **2020**, *32*, 96-109.
[14] C. R. Powell, K. M. Dillon, J. B. Matson, *Biochem. Pharmacol* **2018**, *149*, 110-123.
[15] E. R. DeLeon, G. F. Stoy, K. R. Olson, *Anal. Biochem.* **2012**, *421*, 203-207.
[16] H. Ibrahim, A. Serag, M. A. Farag, *J. Advanced Res.* **2021**, *27*, 137-153.
[17] V. S. Lin, W. Chen, M. Xian, C. J. Chang, *Chem. Soc. Rev.* **2015**, *44*, 4596-4618.
[18] H. M. Smith, M. D. Pluth, *JACS Au* **2023**, *3*, 2677-2691.

[19] A. K. Steiger, S. Pardue, C. G. Kevil, M. D. Pluth, *Journal of the American Chemical Society* **2016**, *138*, 7256-7259.
[20] T. Liang, T. Qiang, L. Ren, F. Cheng, B. Wang, M. Li, W. Hu, T. D. James, *Chem. Sci.* **2022**, *13*, 2992-3001.
[21] W. Liu, D. Bu, H. Zhang, M. Zhang, H. Ren, Z. Li, M. Yu, *Anal. Meth.* **2022**, *14*, 101-105.
[22] L. Li, Z. Lin, Y. Cheng, Y. Tang, Z. Zhang, *Analyst* **2021**, *146*, 7374-7378.
[23] Y. Chen, R. Zhao, C. Tang, C. Zhang, W. Xu, L. Wu, Y. Wang, D. Ye, Y. Liang, *Angew. Chem. Int. Ed.* **2022**, *61*, e202112734.
[24] L. Li, Z. Zhang, *Spectrochim. Acta A Mol. Biomol. Spectrosc.* **2022**, *264*, 120243.
[25] X. Zhao, L. Ning, X. Zhou, Z. Song, J. Zhang, F. Guan, X.-F. Yang, *Anal. Chem.* **2021**, *93*, 4894-4901.
[26] W. Hua, J. Zhao, S. Gou, *Analyst* **2020**, *145*, 3878-3884.
[27] N. Zhang, P. Hu, Y. Wang, Q. Tang, Q. Zheng, Z. Wang, Y. He, *ACS Sensors* **2020**, *5*, 319-326.
[28] Y. Hu, X. Li, Y. Fang, W. Shi, X. Li, W. Chen, M. Xian, H. Ma, *Chem. Sci.* **2019**, *10*, 7690-7694.
[29] J. Liu, M. Zhao, F. Zhao, X. Song, Y. Ye, *Sens. Act. B.* **2023**, *378*, 133131.
[30] A. K. Sharma, M. Nair, P. Chauhan, K. Gupta, D. K. Saini, H. Chakrapani, *Organic. Lett.* **2017**, *19*, 4822-4825.
[31] M. Yao, Y. Lu, L. Shi, Y. Huang, Q. Zhang, J. Tan, P. Hu, J. Zhang, G. Luo, N. Zhang, *Bioactive Materials* **2022**, *9*, 168-182.
[32] X. Zhao, M. Ding, L. Ning, F. Yuan, J. Li, Y. Guo, Y. Mu, J. Zhang, *Acta Materia Medica* **2022**, *1*, 476-485.
[33] F. Yuan, X. He, Y. Lu, L. Ning, X. Zhao, S. Zhang, F. Guan, Y. Guo, J. Zhang, *Anal. Chem.* **2023**, *95*, 6931-6939.
[34] N. Wang, Y. Fang, X. Wang, J. Bai, H. Hua, D. Li, *Chem. Commun.* **2023**, *59*, 8949-8952.
[35] Y. Venkatesh, J. Das, A. Chaudhuri, A. Karmakar, T. K. Maiti, N. D. P. Singh, *Chem. Commun.* **2018**, *54*, 3106-3109.
[36] S. K. Mahato, D. Bhattacherjee, P. Barman, K. P. Bhabak, *J. Mater. Chem. B* **2022**, *10*, 2183-2193.
[37] S. K. Mahato, D. Bhattacherjee, K. P. Bhabak, *Chem. Commun.* **2020**, *56*, 7769-7772.
[38] Y. Zhao, Matthew M. Cerda, M. D. Pluth, *Chem. Sci.* **2019**, *10*, 1873-1878.
[39] B. C. Dickinson, C. Huynh, C. J. Chang, *J. Am. Chem. Soc.* **2010**, *132*, 5906-5915.
[40] M. Hornum, M. W. Mulberg, M. Szomek, P. Reinholdt, J. R. Brewer, D. Wüstner, J. Kongsted, P. Nielsen, *J. Org. Chem.* **2021**, *86*, 1471-1488.
[41] K. Zhou, Y. Yang, T. Zhou, M. Jin, C. Yin, *Dyes Pigments* **2021**, *185*, 108901.
[42] L. Yuan, W. Lin, S. Zhao, W. Gao, B. Chen, L. He, S. Zhu, *Journal of the American Chemical Society* **2012**, *134*, 13510-13523.
[43] P. Greenspan, S. D. Fowler, *J. Lipid Res.* **1985**, *26*, 781-789.
[44] P. Greenspan, E. P. Mayer, S. D. Fowler, *J. Cell Biol.* **1985**, *100*, 965-973.
[45] M. S. A. Abdel-Mottaleb, B. A. El-Sayed, M. M. Abo-Aly, M. Y. El-Kady, *J. Photochem. Photobiol.* **1989**, *46*, 379-390.
[46] C. Bueno, M. L. Villegas, S. G. Bertolotti, C. M. Previtali, M. G. Neumann, M. V. Encinas, *Photochem. Photobiol.* **2002**, *76*, 385-390.
[47] P. Chauhan, P. Bora, G. Ravikumar, S. Jos, H. Chakrapani, *Organic. Lett.* **2017**, *19*, 62-65.
[48] J. L. Bailey, R. D. Cole, *J. Biol. Chem.* **1959**, *234*, 1733-1739.
[49] K. G. Fosnacht, M. M. Cerda, E. J. Mullen, H. C. Pigg, M. D. Pluth, *ACS Chem. Biol.* **2022**, *17*, 331-339.
[50] K. G. Fosnacht, M. D. Hammers, M. S. Earp, A. K. Gilbert, M. D. Pluth, *Chem. Asian J.* **2022**, *17*, e202200426.